Measurements of Diffusion Processes in HEMA–DEGMA Hydrogels by ESR Imaging

S. Schlick,*,† J. Pilar,*,‡ S.-C. Kweon,† J. Vacik,‡ Z. Gao,† and J. Labsky‡

Department of Chemistry, University of Detroit Mercy, Detroit, Michigan 48219, and Institute of Macromolecular Chemistry, Academy of Sciences of the Czech Republic, 162 06 Prague 6, Czech Republic

Received February 22, 1995; Revised Manuscript Received March 27, 1995®

ABSTRACT: The diffusion coefficients of small paramagnetic tracers (nitroxide spin probes) and spin-labeled poly(ethylene oxide) in hydrogels were measured at 300 K, using two-dimensional spatial–spectral ESR imaging (ESRI). The gels were prepared by copolymerization of 2-hydroxyethyl methacrylate (HEMA) and 2-(2-hydroxyethoxy)ethyl methacrylate (DEGMA), in the presence of a fixed molar concentration of glycol dimethacrylate as the cross-linker and 4,4′-azobis(4-cyanopentanoic acid) as the initiator. Variation of the amount of water in equilibrium with the gel was achieved by polymerizing different molar ratios of the monomers. Experimental concentration profiles of the diffusant were measured as a function of time, and each profile was obtained by image reconstruction, from a complete set of projections. The diffusion coefficients were determined by simulating all experimental profiles, using the Fick model of diffusion for an initially confined tracer diffusing into a finite system. The diffusion coefficients depend on the amount of water in the gels. The variation of the diffusion coefficients D with the weight fraction of the copolymer in the gel is consistent with the free volume model. The variation of D with the molecular mass M of the diffusant scales as $M^{-0.8}$ in gels containing ≥67 wt % water and as $M^{-1.4}$ for the gel containing 55 wt % water. The advantages and present limitations of 2D spatial–spectral ESRI for measuring transport properties in polymers are discussed.

I. Introduction

Transport properties of water-soluble low-molecular-weight compounds in hydrogels play an important role in medical applications such as contact lenses and drug delivery systems.[1,2] The hydrogels consist of a polymer network obtained by chemical cross-links and water as solvent. The gels swell until an equilibrium is established between the osmotic forces and the elasticity of the chains, which is determined by the degree of cross-linking. The parameters that affect the diffusion coefficients in hydrogels are the equilibrium water content in the system, the degree of cross-linking, and the hydrophobicity of the network components.

Numerous recent papers on diffusion processes have focused on the study of self-diffusion of solvents and the diffusion of probes, oligomers, and polymers in semidilute polymer solutions. The experimentally determined dependence of the diffusion coefficient D on the molecular mass of the diffusant M and on the polymer concentration c has been compared with theoretical models,[3–10] which predict an $M^{-1/3}$ dependence of the diffusion coefficient for a spherical particle that obeys the Stokes–Einstein equation, an $M^{-1/2}$ dependence in a Θ solvent, an M^{-1} dependence for a Rouse chain, and an M^{-2} dependence for reptating polymer chains in highly entangled systems.[11] The concentration dependence of the diffusion coefficient has been examined by various models, such as the kinetic and free-volume theories.[7] Phillies[3] has recently presented a derivation of the universal scaling law for nondilute polymer solutions from the hydrodynamic scaling model; this model correctly predicts the parameters α, v, and D_0 (which is D at zero polymer concentration) in the expression $D = D_0 \exp(-\alpha c^v)$. It has been concluded[3] that the reptation model, originally proposed for describing the motion of polymers in gels, is not valid for polymer solutions. The different behavior is due to the fact that, even on the short time scale defined by the motion of the probe, chains connected by temporary entanglements in semidilute solutions behave differently compared to permanently cross-linked chains.

The time-dependent local concentration of diffusing species in polymeric systems has been measured by chemical, optical, and radioactive tracers, dynamic light scattering (DLS), fluorescence photobleaching recovery (FPR), and spectroscopic methods.[3,6–10] DLS has been used extensively for the study of polymers in organic solvents. The study of **aqueous** polymer systems, which are becoming increasingly important due to environmental and health concerns, presents additional problems, because of the difficulty of matching the index of refraction of the solvent to that of the matrix. For many aqueous systems, field-gradient spin-echo (PGSE) NMR has emerged as the dominant method. Some of the difficulties expected in the application of this technique have been recently discussed.[12–14] Critical review of the literature reveals that there are problems associated with the estimation of the accuracy for most methods of measurement of diffusion, and discrepancies have been reported even for identical experiments.[9,15]

The effect of paramagnetic species on the nuclear spin–lattice relaxation time T_1 is the basis of a recent elegant method for the measurement of diffusion of paramagnetic species (Cu^{2+}, nitroxide spin probes) in aqueous gels by NMR imaging (NMRI).[16] NMRI has been used to study sorption processes and provides an image of the NMR signal as a function of spatial coordinates, in one, two and three dimensions.[17] These studies have made possible the visualization of motional and structural heterogeneities in cross-linked elastomers and other materials. To the best of our knowlegde, however, such studies have not provided quantitative evaluation of diffusion coefficients.

Electron spin resonance imaging (ESRI) can supply information on the spatial distribution of paramagnetic

* Authors to whom correspondence should be addressed.
† University of Detroit Mercy.
‡ Academy of Sciences of the Czech Republic.
® Abstract published in *Advance ACS Abstracts,* July 15, 1995.

0024-9297/95/2228-5780$09.00/0

molecules in a sample and has been used successfully for the measurement of translational diffusion.[18–20] Diffusion coefficients of paramagnetic diffusants can be deduced from an analysis of the time dependence of concentration profiles along a selected axis of the sample. The determination of diffusion coefficients of spin probes in liquid crystals and model membranes has been described in an important series of papers by Freed and co-workers.[21–26] Recent improvements in the technique of dynamic imaging of diffusion by ESR[22,23] has allowed the measurement of diffusion coefficients of the order of 10^{-7} cm^2 s^{-1} in 1 h.

In our laboratory we have applied ESRI in two dimensions (spectral–spatial) as a method for real-time representation of structural imhomogeneities and dynamics in polymer blends, ionomers, composites and cross-linked polymer gels.[27,28] Projections of the sample taken in a range of magnetic field gradients are used to reconstruct a 2D spatial–spectral image that consists of the ESR spectrum along the chosen spatial coordinate. The method requires long measurement times but can supply not only the concentration profile of the diffusant but also the line shape of the ESR spectrum of the diffusant in each slice of the sample perpendicular to the direction of the gradient. This approach makes possible the determination of translational **and** rotational diffusion of the spin-labeled diffusant along the spatial axis of the sample in one experiment. We are currently applying this method for the study of transport properties of nitroxide spin probes and spin-labeled polymers in solutions of linear polystyrene (PS) in toluene and in cross-linked PS gels swollen by various solvents.[29] To the best of our knowledge, diffusion in polymers by ESRI has been reported in only one recent paper,[26] where the imaging method used did not provide spectral information.

In this paper we present the application of two-dimensional spectral–spatial ESRI for measuring the translational diffusion of nitroxide spin probes and spin-labeled poly(ethylene oxide) (SLPEO) in hydrogels based on slightly hydrophilic copolymers of 2-hydroxyethyl methacrylate (HEMA) and 2-(2-hydroxyethoxy)ethyl methacrylate (DEGMA). The copolymers are neutral and have excellent biological tolerance and good mechanical properties even at high water content (>60%). For these reasons the gels are especially useful for production of contact lenses. Data on the transport of oxygen, low-molecular-weight water-soluble drugs and metabolites across the gels are important for this application.

The transport properties of different solutes in HEMA-based hydrogels have been studied by measuring the permeability of membranes prepared from the copolymers.[30–33] The determination of the diffusion coefficients from these measurements is complicated by the need to determine independently the partition coefficients of the diffusant for the system membrane–solvent; such information has been obtained only for inorganic salts. The main conclusions derived from such studies are the increased permeability with increasing water content in the gels and with decreasing degree of cross-linking and the higher permeability of inorganic salts across ampholytic membranes (that contain the same amounts of weak acidic and weak basic groups) compared with neutral membranes.

This study was initiated with two main objectives. First, we were interested in exploring the potential of 2D spatial–spectral ESRI as a method for measuring diffusion in hydrogels. Second, we wanted to detect the effect of the network composition and water content on the diffusion rates of small neutral and ionic diffusants and of polymers. On the basis of the results presented below, it appears that the development of ESRI is important for the evaluation of materials suitable in medical and industrial applications.

Scheme 1

Monomers:

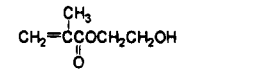

2-hydroxyethylmethacrylate (HEMA)

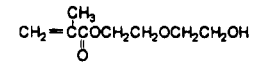

Diethylene glycol monomethacrylate (DEGMA)

Initiator

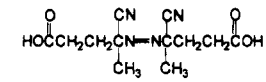

4,4'-azobis(4-cyanopentanoic acid)

Crosslinker

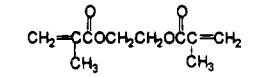

Ethylene glycol dimethacrylate

II. Experimental Section

Sample Preparation. The monomer 2-hydroxyethyl methacrylate (HEMA) was purified by column distillation (approximately five theoretical plates) to a bp of 323–325 K at 0.1 torr; the residual content of glycol dimethacrylate (0.12 mol %) was determined by gas chromatography. 2-(2-Hydroxyethoxy)ethyl methacrylate (DEGMA) and the cross-linker glycol dimethacrylate (Rohm, Germany) were distilled before use. The reaction mixture composed of HEMA, DEGMA, glycol dimethacrylate (0.32 mol %), the initiator 4,4'-azobis-(4-cyanopentanoic acid) (Fluka, 0.5 mol %), and water (at amounts corresponding to the equilibrium content in the gel) was bubbled with nitrogen for 15 min at room temperature, filled in glass capillary tubes (1–2 mm i.d.), and copolymerized at 333 K for 24 h in a closed container. Three gel systems were prepared, containing 100, 80, or 50 mol % DEGMA, respectively; the notation is DE100, DE80, and DE50. The corresponding equilibrium water contents of 75, 67, and 55 wt % were determined gravimetrically. All samples were stored in the water bath at ambient temperature before use.

For the imaging measurements, the capillaries containing the aqueous gels were cut into pieces ≈8 mm long, and ≈1 mm of the glass tube was removed at one end. The exposed gel was then soaked for 5–10 min at ambient temperature with an aqueous solution of the paramagnetic diffusant; typical concentrations of the diffusant were 0.1 mol/L. The samples were flame-sealed inside thin wall Pyrex sample tubes (3–4 mm o.d.) and positioned vertically in the cavity of the ESRI spectrometer, with the layer soaked by the diffusant on top. Diffusion processes were measured at 300 K, using the Bruker variable temperature flow system 4111VT.

Diffusants. Three diffusants were studied. The ionic probe 4-(trimethylammonio)-2,2,6,6-tetramethylpiperidine-*N*-oxyl iodide (TMATEMPOI, MW 211) was purchased from Molecular Probes Inc., Portland, OR. The neutral probe perdeuterio-2,2,6,6-tetramethyl-4-piperidone-*N*-oxyl (PDTEMPONE, MW 170) was synthesized according to a published procedure.[34] Spin-labeled poly(ethylene oxide) (SLPEO, MW 1831) was prepared from PEO (Fluka, MW 1500) by attachement of 3-carboxy-2,2,5,5-tetramethylpyrrolidine-*N*-oxyl[35] to both OH end groups of the polymer.[36] The materials used for the preparation of the gels and the diffusants are shown in Schemes 1 and 2, respectively.

ESR Imaging Spectrometer. The ESR imaging system in Detroit consists of the Bruker 200D ESR spectrometer

Scheme 2. Diffusants

Perdeuterio-2,2,6,6-tetramethyl-4-piperidone-N-oxyl (PDTEMPONE)

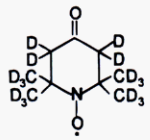

4-trimethylammonio-2,2,6,6-tetramethylpiperidine-N-oxyl iodide (TMATEMPOI)

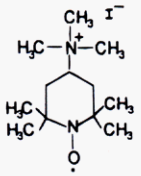

Spin-labelled poly(ethylene oxide) (SLPEO)

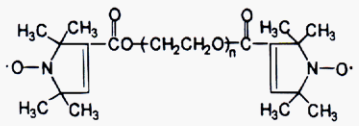

equipped with two Lewis Coils (George Associates, Berkeley, CA, type 503D) and two regulated dc power supplies (Kikusui Electronic Corp., Japan, Model PAE 35-30). The two sets of coils, each consisting of a figure-eight coil, were fixed on the poles of the spectrometer magnet and can supply a maximum linear field gradient of ≈320 G/cm in the direction parallel to the external magnetic field (z axis), or ≈250 G/cm in the vertical direction (along the long axis, x, of the microwave cavity), with a control voltage of 20 V applied to each power supply. The magnetic field gradient was measured by taking ESR spectra of a sample consisting of two small specks of 2,2-diphenyl-1-picrylhydrazyl (DPPH) fixed at a distance of 1 cm along the direction of the gradient, on the surface of a quartz tube (10 mm o.d.), in a range of gradients generated with control voltages ranging from 0 to 20 V; no departure from linearity was detected for gradients along the x or z axis. The coils were positioned so that the zero point of the gradient field coincided with the center of the microwave cavity.

The imaging spectrometer was interfaced to a 386 AST PC equipped with software developed in our lab and designed to control the magnitude of the field gradient by set input voltages to the dc power supplies, and to collect the data.[27] The data were processed and simulated with a NEC READY 486 PC, using the software MATLAB. The results can be presented with the HP Laser Printer 4L, HP ColorPro Plotter, and HP DeskJet 550C Color Printer.

III. Data Acquisition

The progress of diffusion was followed from spatial–spectral images measured as a function of time. Each image was reconstructed from a complete set of projections taken as a function of the magnetic field gradient,[37,38] using a convoluted back-projection algorithm.[27] The number of points for each projection (4096) was kept constant. The maximum experimentally accessible projection angle α_{max} can be calculated from the maximum gradient G_{max} according to $\tan \alpha_{max} = (L/\Delta H)G_{max}$, where ΔH is the spectral width in the absence of gradient ($\alpha = 0$). The maximum sweep width $SW_{max} = \sqrt{2}\, \Delta H/\cos \alpha_{max}$.

For ΔH = 54.5 G (which was broad enough for motionally narrowed ESR spectra of the two smaller spin probes and the spin-labeled polymer used as diffusants), a sample length of 1.1 cm, and a maximum field gradient of 200 G/cm along the vertical axis, we obtain $\alpha_{max} = 76.1°$ and $SW_{max} = 317.2$ G. A complete set of data for one image consisted of 65 projections,

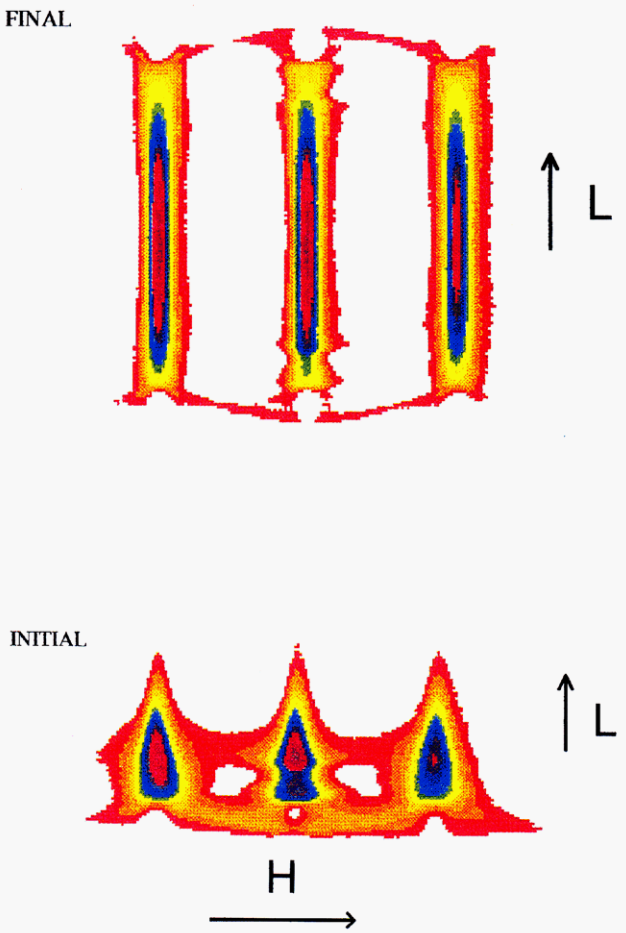

Figure 1. Two-dimensional contour plots of the initial and final spatial–spectral images for the diffusion of TMATEMPOI in DE80 at 300 K.

taken for gradients corresponding to equally spaced increments of α in the range −90 to +90°; of these projections, 55 are experimentally accessible projections and 10 are projections for missing angles (for α in the intervals 76.1–90° and −76.1 to −90°). The projections at the 10 missing angles were assumed to be the same as those at the maximum experimentally accessible angle α_{max}.

Each projection required three scans to reach an acceptable signal-to-noise ratio, and each scan was obtained with a 10 s scan time, 2 mW microwave power, 1 G modulation, and a time constant of 10 ms for the smaller probes and 50 ms for SLPEO. The spectrometer gain was 2000–5000 in most cases, and 1×10^5 for measurements involving the slow diffusion of SLPEO in DE50. The acquisition of the projections necessary for each image at a given time t required ≤30 min. These conditions imply that the method may be used for the study of relatively slow diffusion processes, when the change of the concentration profile during acquisition time is negligible.

The first-derivative ESR spectra taken in the presence of gradients were numerically integrated and multiplied by the square of the sweep width, in order to obtain a constant integrated intensity, as required by the image reconstruction algorithm,[37] and the 4096 points collected for each spectrum were compressed by averaging to 256 points. The reconstruction algorithm produced a three-dimensional spatial–spectral–intensity image of the diffusant distribution in the sample consisting of 256 × 256 points. The concentration of the diffusant at each point of the spatial axis of a sample at a given time was

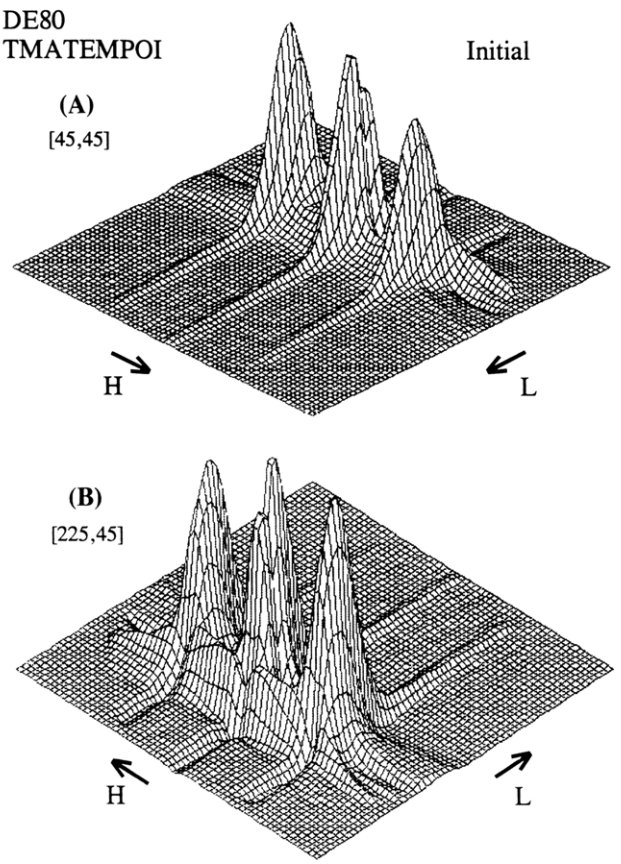

Figure 2. Perspective plots of the three-dimensional spatial–spectral–intensity initial images for the diffusion of TMATEMPOI in DE80 at 300 K, from two opposite directions, in (A) and (B), respectively. The viewing angles θ and ϕ in the L (spatial), I (intensity), and H (magnetic field) axes are given in square brackets. The length scale (L) is along the direction from the top of the sample soaked with diffusant to the bottom; the magnetic field scale is along the increasing field. In the two images the length range is 15.6 mm and the magnetic field range is 77 G.

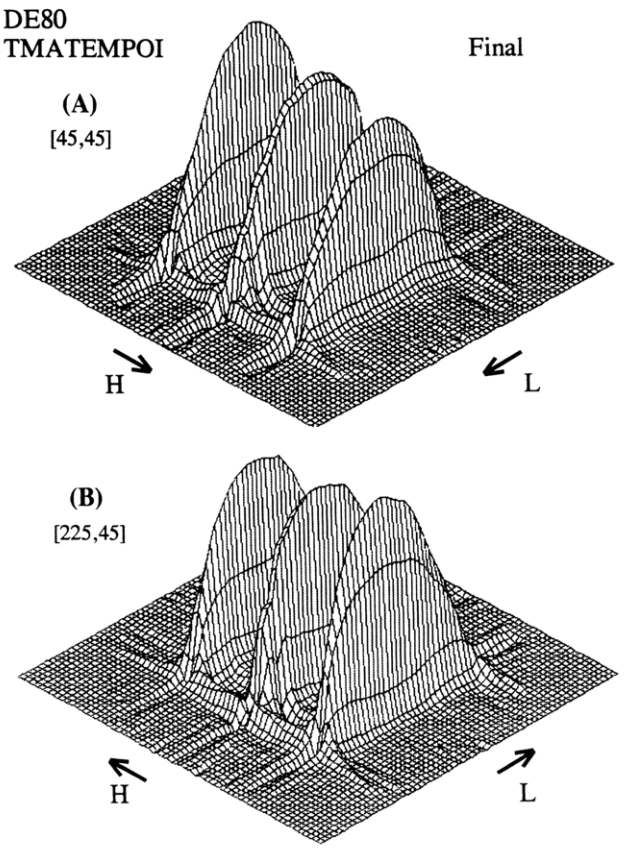

Figure 3. Perspective plots of the three-dimensional spatial–spectral–intensity final images for the diffusion of TMATEMPOI in DE80 at 300 K, from two opposite directions, in (A) and (B), respectively. For more details see Figure 2.

obtained by integrating the ESR spectra at this point along the spectral (magnetic field) axis, thus creating the corresponding experimental concentration profile.

IV. Results

The diffusion of the two spin probes TMATEMPOI and PDTEMPONE and of the spin-labeled polymer SLPEO in the DE100, DE80, and DE50 gels was imaged at 300 K.

In Figure 1 we present two-dimensional color contour plots of the initial and final spatial–spectral images for the diffusion of TMATEMPOI in DE80. We note the initial confinement of the signal in a limited region of space, and the homogeneous distribution of the signal in the sample in the final image. Detailed line shapes can be observed in the perspective presentations of the spatial–spectral images, shown in Figures 2 and 3 for the initial and final stages, respectively, of the TMATEMPOI diffusion in DE80. In these figures, and in all the perspective plots shown below, we indicated in square brackets the viewing angles θ and ϕ in the axes system L (spatial), I (intensity), and H (spectral) coordinates. Each pair was constructed with constant ϕ values, but the θ values were 45 and 225° (45 + 180°) in parts A and B of each figure, respectively, in order to visualize opposite views of the object. Broader spectral lines in a thin layer are seen clearly in the initial image shown in Figure 2B and are assigned to spin probes located in the top layer of the sample, which contains a larger concentration of the diffusant. The appearance of these lines demonstrates the high **spatial** resolution of the method and its sensitivity to the **spectral** line shapes, which are determined by the dynamics of the spin probe. The broad signals are superimposed on imaging artifacts, which are due to the sharp edges of the sample and also to the approximations involving the projections at missing angles. The broad signals become less visible as the diffusion process advances, as seen in the final image shown for this system in Figure 3B, because the spin probes in the top layer become distributed along the entire length of the sample.

The perspective plots presented in Figures 4 and 5 show the slower rotational dynamics (higher differences in the heights of the three spectral components) for the same spin probe in DE50, compared with the results obtained for the DE80 gel (Figures 2 and 3). The broad spectra in the top layer of the sample are even more distinct in Figures 4 and 5. Significant narrowing of spectral lines for the completely deuteriated probe PDTEMPONE in DE50 is clearly seen in Figure 6, especially when comparing with the corresponding images of the protiated small probe, Figure 4. The two images shown in Figure 7, for the initial stage of diffusion of SLPEO in DE50, indicate the slow rotational mobility of the spin label attached to the polymer chain.

A complete series of experimental concentration profiles for the diffusion of TMATEMPOI in DE80 is presented in Figure 8A. All experimental profiles taken for a particular sample at different times were splined using a cubic spline, with 16 control points. The part of the profiles corresponding to the sample length was selected; the experimental splined profile in the L scale

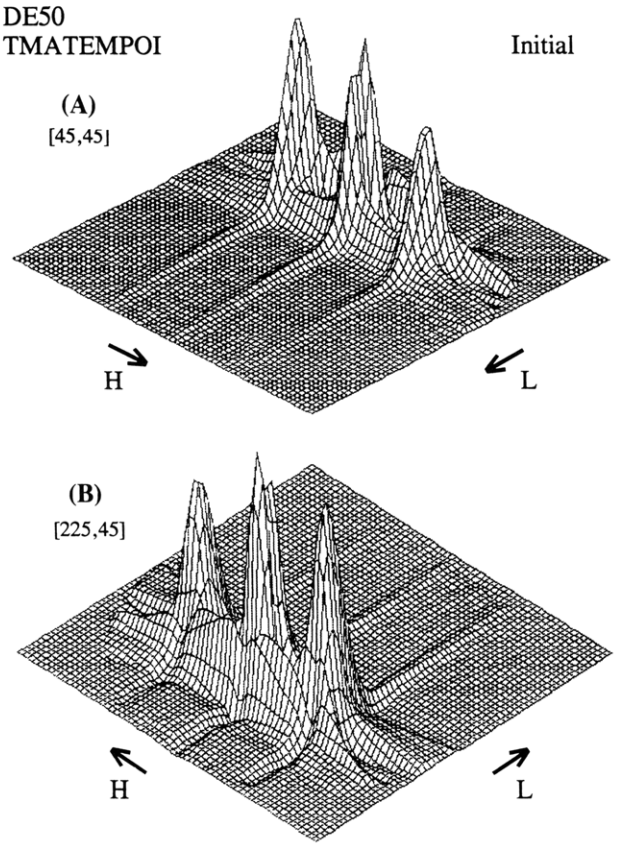

Figure 4. Perspective plots of the three-dimensional spatial–spectral–intensity initial images for the diffusion of TMATEMPOI in DE50 at 300 K, from two opposite directions, in (A) and (B), respectively. For more details see Figure 2.

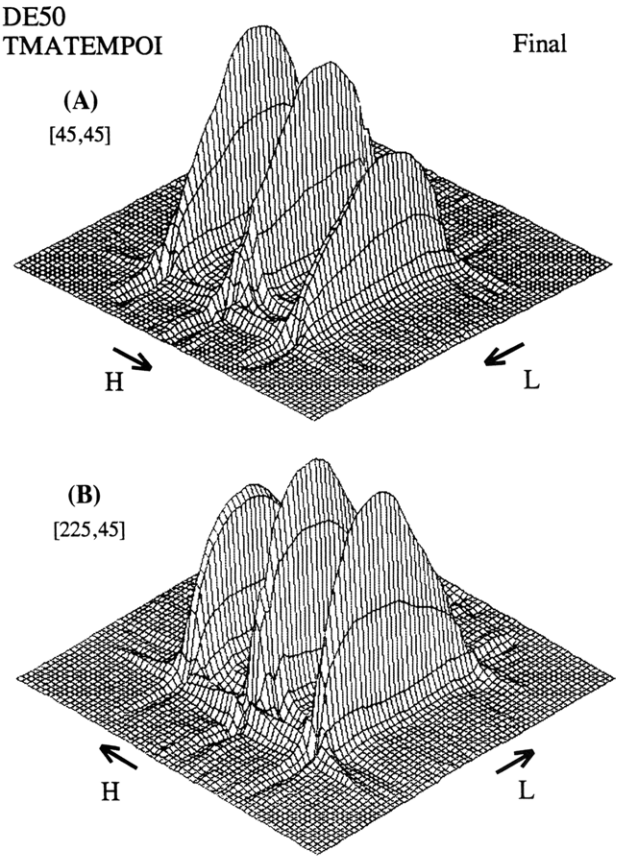

Figure 5. Perspective plots of the three-dimensional spatial–spectral–intensity final images for the diffusion of TMATEMPOI in DE50 at 300 K, from two opposite directions, in (A) and (B), respectively. For more details see Figure 2.

generated in this manner is shown in Figure 8B for the diffusion of TMATEMPOI in DE80. This type of data was obtained for each of the probe–gel systems that was studied.

V. Determination of Diffusion Coefficients by Simulation of Concentration Profiles

The diffusion coeficients were determined by comparing the experimental splined concentration profiles (such as that shown in Figure 8B) with calculated profiles obtained on the basis of Fick's laws of diffusion.[39] In our sample, the diffusant is initially confined in the region $0 < x < h$, and the spin probes diffuse into a finite system of length l. The boundary conditions at $t = 0$ are $C{=}C_0$ for $x \leq h$, and $C = 0$ for $x > h$. An additional condition is $\delta C/\delta x = 0$ at $x = l$ (no flow of the diffusion substance through the closed part of the tube). The solution for this sample configuration is given in eq 1

$$C(x,t) = \frac{1}{2}C_0 \sum_{n=-\infty}^{+\infty} \left\{ \operatorname{erf} \frac{h + 2nl - x}{2\sqrt{Dt}} + \operatorname{erf} \frac{h - 2nl + x}{2\sqrt{Dt}} \right\} \tag{1}$$

where

$$\operatorname{erf}(x) \equiv \frac{2}{\sqrt{\pi}} \int_0^x \exp[-\xi^2]\, d\xi$$

For each time-dependent concentration profile we simulated 21 equally spaced points using eq 1, with five terms ($n = -2, \ldots, 2$) in the summation needed for convergence. The 21 calculated points were then multiplied by the **final experimental** concentration profile of the sample, measured when a homogeneous distribution of the diffusant in the sample was reached. In this way the sensitivity of the ESR cavity along the (vertical) diffusion direction was taken in consideration for each specific position of the sample in the cavity. The three parameters D, h, and C_0 can be varied for each experimental profile, until the best fit is reached. In practice, the thickness of initial layer of the diffusant (h) was determined by simulating the profiles taken in the earliest stage of diffusion and the h value was then kept constant during the simulation of all profiles for a given sample. The initial concentration was slightly varied in some cases, due to the uncertainty in splining noisy experimental concentration profiles. In Figure 8C we present the simulated concentration profiles for the diffusion of TMATEMPOI in DE80, which are in excellent agreement with the experimental splined profiles given in Figure 8B.

Each simulated concentration profile gives a value for the diffusion coefficient D. The number of D values for a given system is therefore equal to the number of images, typically 6–10. We observed a slight increase of D with time for all samples studied and are currently investigating whether this effect is due to a systematic experimental error or non-Fickian diffusion. For the moment, we considered this effect as an experimental error and deduced the diffusion coefficients as an average of all values determined by fitting profiles of a series taken for the sample in the entire diffusion time range; the experimental error was estimated to be ±10–15%. The D values thus calculated are given in Table 1.

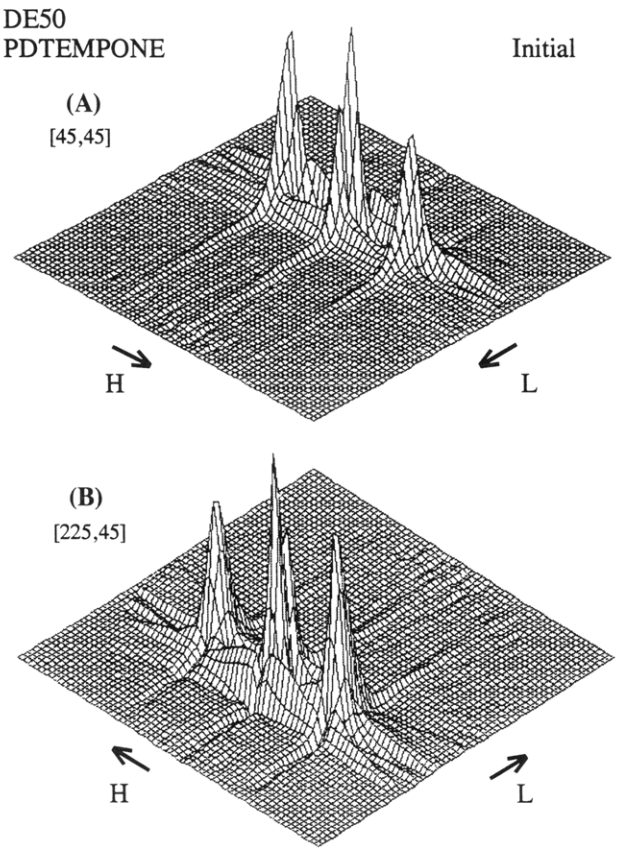

Figure 6. Perspective plots of the three-dimensional spatial–spectral–intensity initial images for the diffusion of PDTEMPONE in DE50 at 300 K, from two opposite directions, in (A) and (B), respectively. For more details see Figure 2.

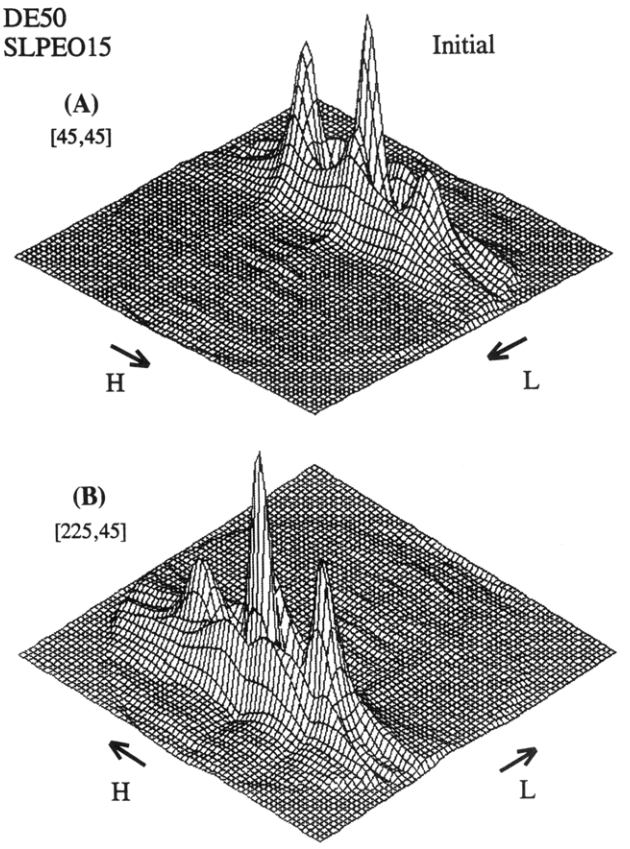

Figure 7. Perspective plots of the three-dimensional spatial–spectral–intensity initial images for the diffusion of SLPEO in DE50 at 300 K, from two opposite directions, in (A) and (B), respectively. For more details see Figure 2.

Typical times for attaining an equilibrium concentration profile for the small probes were 1–2 days. A very slow diffusion of SLPEO was followed in DE50 for more than 2 weeks. The diffusion coefficient of the order of 0.1×10^{-7} cm^2/s was estimated by analyzing experimental profiles measured for this sample, using the final profile of a similar sample. Additional experiments showed a very slow diffusion of SLPEO prepared from PEO of MW 3000 in DE80, and practically no diffusion of TMATEMPOI in DE00 (pure cross-linked HEMA gel).

VI. Discussion

Inspection of Table 1 indicates that the diffusion coefficients D decrease with decreasing water content in the gel, and with increasing molecular mass of the diffusant. The decrease of D with decreasing water content is very similar for the two smaller probes, but much more pronounced for SLPEO.

The dependence of solvent diffusion coefficients on the concentration of polymers in solution or gels has been often found to follow the free volume theory.[40,41] At polymer concentrations lower than ≈50% by weight, a particularly simple expression has been suggested,

$$\log(D/D_0) = Aw_2/(1 - w_2) \qquad (2)$$

where D_0 is the diffusion coefficient in the absence of polymer, A is a system-dependent constant, and w_2 is the weight fraction of the polymer.[7] Plots of our data in log D vs $w_2/(1 - w_2)$ axes are presented in Figure 9. The points for each diffusant fit well the expected linear dependence (the correlation factors are 0.996, 0.999, and 0.988 for TMATEMPOI, PDTEMPONE, and SLPEO, respectively). In Figure 9 we also present, for comparison, the data that Yasunaga and Ando[42] have obtained for the diffusion of water in poly(methacrylic acid) (PMAA) gels, where the water content was varied by different degrees of cross-linking. It appears that the larger diffusants are significantly more sensitive to the amount of water in the gels.

In order to examine the scaling behavior of D with the molecular mass ($D \sim M^{-\alpha}$) for the hydrogels, we evaluated the exponent α for the neutral probes PDTEMPONE and SLPEO. For the DE100 and DE80 gels, α = 0.8; this value is in agreement with the data of Piton et al. for the diffusion of solvents and styrene oligomers in polystyrene solutions[9] and with the data of Bu and Russo for the diffusion of dextrans in aqueous (hydroxypropyl)cellulose.[10] For the hardest gel (DE50), however, α = 1.4. It appears that the mechanism of diffusion changes dramatically for a relatively small change in the water content (from 67 to 55 wt %). A gradual change of α with the polymer concentration has also been observed for the diffusion coefficients of PS oligomers in PS solutions in benzene at 298 K.[9] As in this study, α is in the range $^1/_2$–2. It is interesting to note that Martin[43] has proposed a different scaling law, α = 1.8, for the case of diffusing chains that are different from the gel network, in the presence of a good solvent. This behavior has been verified for the diffusion of PS in methyl methacrylate (MMA)–ethylene dimethacrylate (EDMA) gels in toluene.[44]

The D values for the polar probe are higher in a given gel than those of the neutral small probe, although its molecular mass is slightly larger (211 vs 170). As found previously for the diffusion of neutral and charged probes in various gels,[16] it seems that molecular interactions are important in determining transport proper-

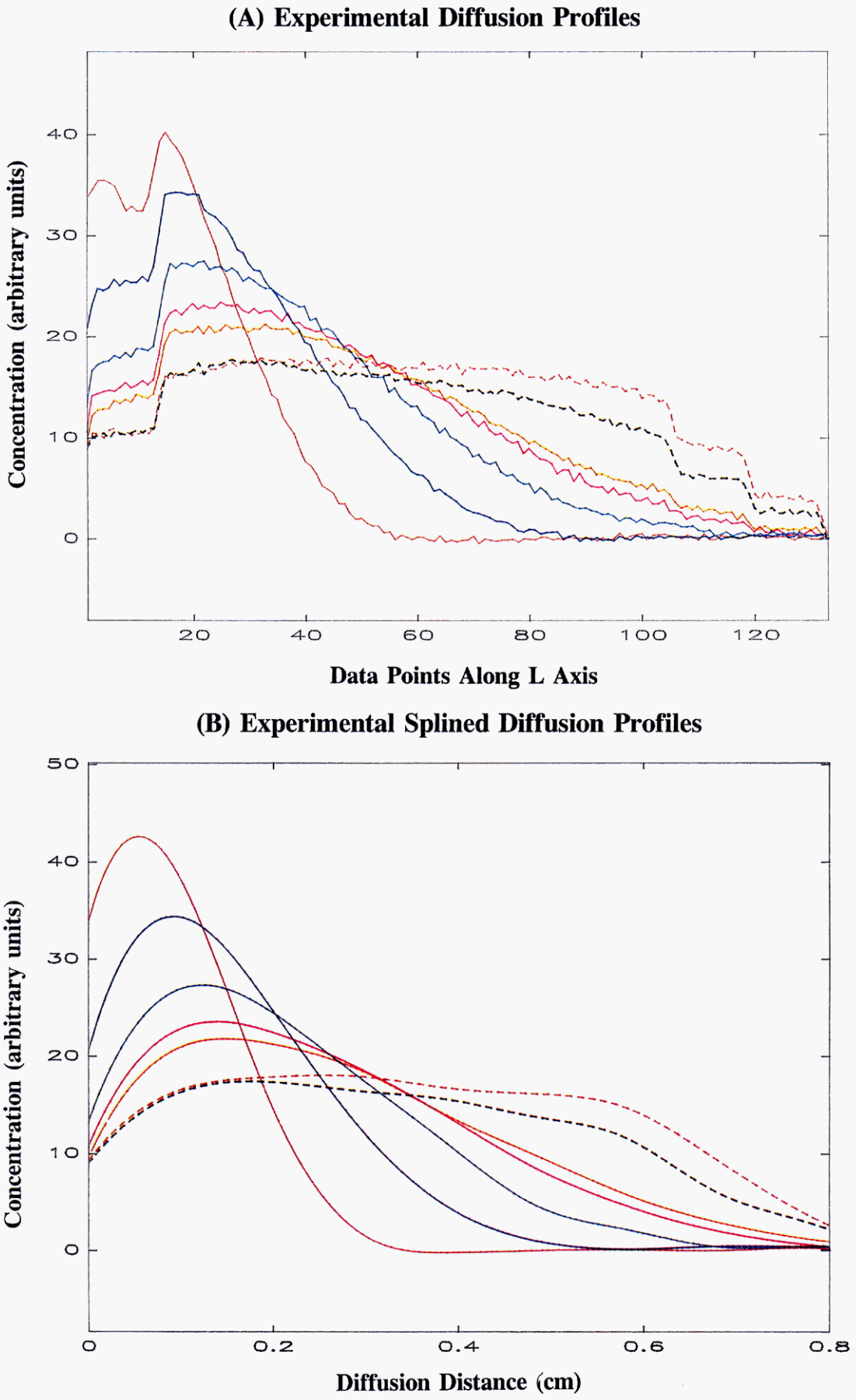

Figure 8 (continued)

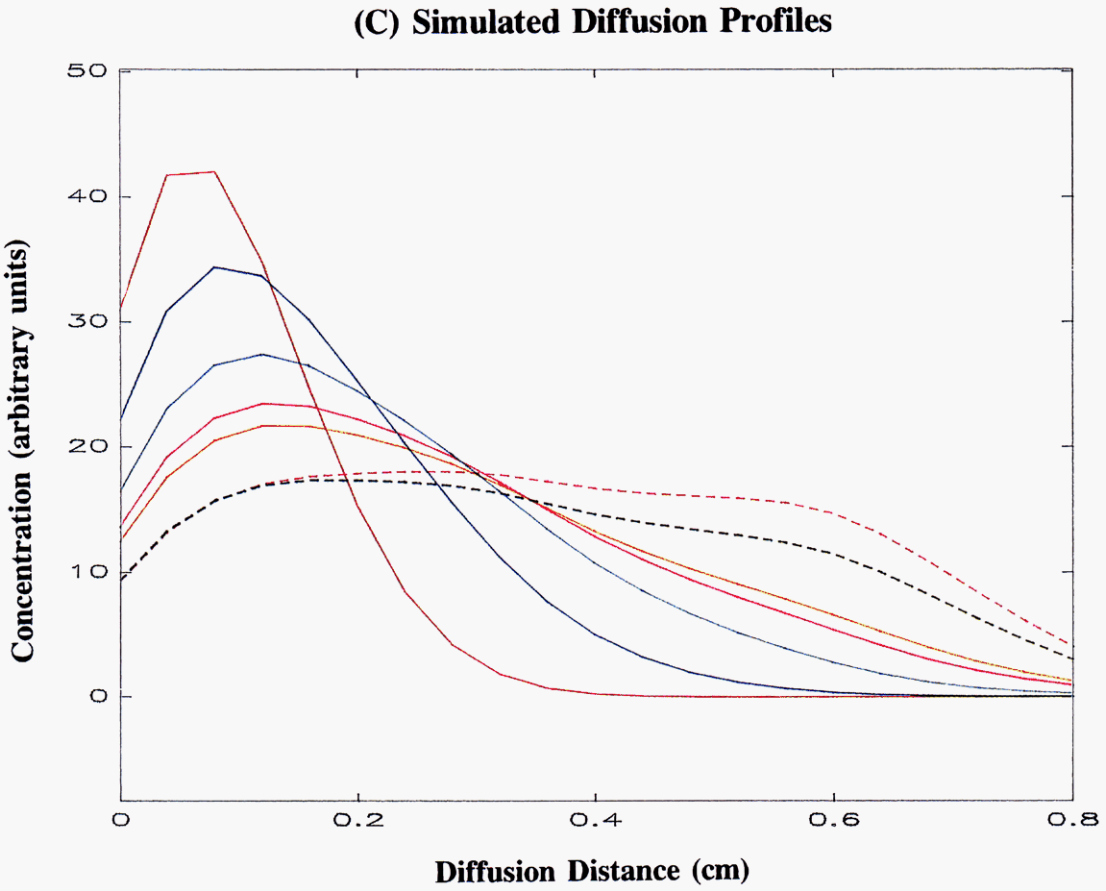

Figure 8. Complete set of experimental (A), splined (B), and calculated (C) concentration profiles for the diffusion of TMATEMPOI in DE80 at 300 K. Consecutive experimental images were taken at t = 4940, 12 140, 22 940, 33 740, 40 940, 77 300, and 112 220 s. The abscissa in (A), is the number of points corresponding to the actual length of the sample, out of a total of 256 points collected. The abscissa in (B) and (C) is the length of the sample tube.

Table 1. Diffusion Coefficients (in units of 10^{-7} cm^2 s^{-1}) at 300 K of Three Diffusants in HEMA–DEGMA Hydrogels

sample (water content, wt %)	TMATEMPOI (M = 211)	PDTEMPONE (M = 170)	SLPEO (M = 1832)
DE100 (75)	24 ± 4	24 ± 4	3.4 ± 0.5
DE80 (67)	17 ± 3	13 ± 2	1.8 ± 0.3
DE50 (55)	6 ± 1	3 ± 1	≈0.1

ties in gels.

The results presented above indicated that 2D spatial–spectral ESRI can provide quantitative data on transport properties of paramagnetic diffusants in hydrogels. The method we use for the simulation of experimental profiles provides a value of the translational diffusion coefficient for each stage in the diffusion process, making it possible to estimate the experimental error. The concentrations of the spin probes, especially the perdeuteriated ones, are low, so that the values of the diffusion coefficients can be considered close to those obtained by extrapolation to zero concentration. Moreover, information on rotational diffusion can also be obtained, from the ESR line shapes as a function of the spatial dimension. Although this potential has not been explored in this study, we anticipate making use of this possibility in other systems. Temperature variation will also extend the range of data in the spectral and spatial dimensions. The most serious drawback of the method we use now is the limited range of diffusion coefficients that can be measured and the long measurement times. We are currently working on modifying the data acquisition and image reconstruction algorithm, on using other paramagnetic tracers besides nitroxides, and on applications to systems where the ESR spectrum of the tracer changes as it diffuses.

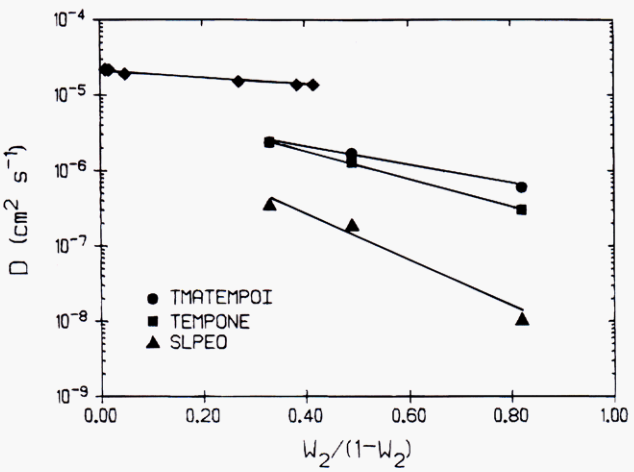

Figure 9. Dependence of diffusion coefficients D of TMATEMPOI (●), PDTEMPONE (■) and SLPEO (▲) on $w_2/(1 - w_2)$, where w_2 is the weight fraction of the network in the gels swollen at equilibrium by water. Diffusion coefficients of pure water in PMAA aqueous networks[39] are also indicated (◆).

VII. Conclusions

The diffusion coefficients of small paramagnetic molecules (spin probes) and spin-labeled polymers in cross-linked gels swollen by water were measured at 300 K, using two-dimensional spatial–spectral ESR imaging (ESRI). The gels were prepared by copolymerization of 2-hydroxyethyl methacrylate (HEMA) and 2-(2-hydrox-

yethoxy)ethyl methacrylate (DEGMA), in the presence of glycol dimethacrylate as the cross-linker. The networks were prepared with a fixed molar concentration of the cross-linking agent; variation of the amount of water in equilibrium with the polymer was achieved by polymerizing different molar ratios of the monomers.

Experimental concentration profiles of the diffusant in the sample were measured as a function of time, and each profile was obtained by image reconstruction, from a complete set of projections taken in a range of magnetic field gradients. The diffusion coefficients were determined by simulation of the experimental diffusion profiles as a function of time, using the Fick model of diffusion, for an initially confined tracer that diffuses into a finite system.

The diffusion coefficients depend on the amount of water in the gels, with the highest changes observed for the spin-labeled polymer. The variation of the diffusion coefficients D with the network fraction is consistent with the free volume model. The variation of D scales with $M^{-0.8}$ in gels containing ≥ 66 wt % water, but the scaling changes to $M^{-1.4}$ for the gel containing 55 wt % water, suggesting a change in the diffusion mechanism with water content. At present, the 2D ESRI method presented above is applicable for the case of relatively slow diffusion, with D in the range $10^{-6}-10^{-8}$ cm^2/s.

Acknowledgment. This research has been supported by NSF (Polymers Program), AAUW, the U.S.-Czech Science and Technology Program, and the Grant Agency of the Czech Republic. We are grateful to K. Ohno for his assistance and encouragement in the early stages of ESR imaging in our laboratory and to T. M. Lodge for illuminating discussions.

References and Notes

(1) *Controlled Drug Delivery*; Robinson, J. R., Lee, V. H. L., Eds.; Marcel Dekker Inc.: New York and Basel, 1987.
(2) *Ophthalmic Drug Delivery Systems*; Mitra, A. K., Ed.; Marcel Dekker Inc.: New York, Basel, Hong Kong, 1993.
(3) Phillies, G. D. J. *J. Phys. Chem.* **1989**, *93*, 5029.
(4) Lodge, T. P.; Wheeler, L. M. *Macromolecules* **1986**, *19*, 2983.
(5) Wheeler, L. M.; Lodge, T. P.; Hanley, B.; Tirrell, M. *Macromolecules* **1987**, *20*, 1120.
(6) Furukawa, R.; Arauz-Lara, J. L.; Ware, B. R. *Macromolecules* **1991**, *24*, 599.
(7) Waggoner, R. A.; Blum, F. D.; MacElroy, J. M. D. *Macromolecules* **1993**, *26*, 6841.
(8) Nystrom, B.; Walderhaug, H.; Hansen, F. K. *J. Phys. Chem.* **1993**, *97*, 7752.
(9) Piton, M. C.; Gilbert, R. G.; Chapman, B. E.; Kuchel, P. W. *Macromolecules* **1993**, *26*, 4472.
(10) Bu, Z.; Russo, P. S. *Macromolecules* **1994**, *27*, 1187.
(11) de Gennes, P. G. *Scaling Concepts in Polymer Physics;* Cornell University Press: Ithaca, NY, 1979.
(12) Lucas, A. J.; Gibbs, S. J.; Jones, E. W. G.; Peyron, M.; Derbyshire, J. A.; Hall, L. D. *J. Magn. Reson.* **1993**, *A 104*, 273.
(13) Snaar, J. E. M.; Van As, H. *J. Magn. Reson.* **1993**, *A102*, 318.
(14) Ilyina, E.; Daragan, V. *Macromolecules* **1994**, *27*, 3759.
(15) Pickup, S.; Blum, F. D. *Macromolecules* **1989**, *22*, 3961.
(16) Balcom, B. J.; Fischer, A. E.; Carpenter, A.; Hall, L. D. *J. Am. Chem. Soc.* **1993**, *115*, 3300.
(17) Rana, M. A.; Koenig, J. L. *Macromolecules* **1994**, *27*, 3727. This paper gives a lucid description of the use of NMRI to study sorption of solvents in complex polymeric systems and lists relevant references.
(18) Galtseva, E. U.; Yakimchenko, O. Y.; Lebedev, Y. S. *Chem. Phys. Lett.* **1983**, *99*, 301.
(19) Berliner, L. J.; Fujii, H. *J. Magn. Reson.* **1986**, *69*, 68.
(20) Demsar, F.; Swartz, H. M.; Schara, M. *Magn. Reson. Med. Biol.* **1988**, *1*, 17.
(21) Hornak, J. P.; Moscicki, J. K.; Schneider, D. J.; Freed, J. H. *J. Chem. Phys.* **1986**, *84*, 3387.
(22) Moscicki, J. K.; Shin, Y. K.; Freed, J. H. In *EPR Imaging and in Vivo EPR*; Eaton, G. R., Eaton, S. S., Ohno, K., Eds.; CRC Press, Inc.: Boca Raton, FL 1991; Chapter 19, p 189.
(23) Moscicki, J. K.; Shin, Y. K.; Freed, J. H. *J. Chem. Phys.* **1993**, *98*, 634.
(24) Shin, Y.-K.; Ewert, U.; Budil, D. E.; Freed, J. H. *Biophys. J.* **1991**, *59*, 950.
(25) Freed, J. H. *Annu. Rev. Biophys. Biomol. Struct.* **1994**, *23*, 1.
(26) Xu, D.; Moscicki, J. K.; Budil, D. E.; Freed, J. H. *Polym. Prepr. (Am. Chem. Soc., Div. Polym. Chem.)* **1994**, *35*, 809.
(27) Kweon, S.-C. M.Sc. Thesis, University of Detroit Mercy, 1993.
(28) Kweon, S.-C.; Gao, Z.; Eagle, P.; Schlick, S.; Labsky, J.; Pilar, J. *Polym. Mater. Sci. Eng.* **1994**, *71*, 169.
(29) Gao, Z.; Kweon, S.-C.; Eagle, P.; Schlick, S.; Pilar, J., to be published.
(30) Kopeček, J.; Vacík, J.; Lím, D. *J. Polym. Sci., Polym. Chem. Ed.* **1971**, *9*, 2801.
(31) Kopeček, J.; Vacík, J. *Collect. Czech. Chem. Commun.* **1973**, *38*, 854.
(32) Dabrovska, L.; Praus, R.; Stoy, V.; Vacik, J. *J. Biomed. Mater. Res.* **1978**, *12*, 591.
(33) Yasuda, H.; Lamaze, C. E.; Peterlin, A. *J. Polym. Sci., Polym. Chem. Ed.* **1971**, *9*, 1117.
(34) Chiarelli, R.; Rassat, A. *Tetrahedron* **1973**, *29*, 3639.
(35) Rozantsev, E. G.; Krinitskaya, L. A. *Tetrahedron* **1965**, *21*, 491.
(36) Tormala, P.; Lattila, H.; Lindberg, J. J. *Polymer* **1973**, *14*, 481.
(37) Maltempo, M. M.; Eaton, S. S.; Eaton, G. R. In *EPR Imaging and in Vivo EPR*; Eaton, G. R., Eaton, S. S., Ohno, K., Eds.; CRC Press, Inc.: Boca Raton, FL 1991; Chapter 13, p 135.
(38) Maltempo, M. M.; Eaton, S. S.; Eaton, G. R. *J. Magn. Reson.* **1987**, *72*, 449.
(39) Crank, J. *The Mathematics of Diffusion*; Clarendon Press: Oxford, U.K., 1993.
(40) Vrentas, J. S.; Duda, J. L.; Ling, H. C. *J. Polym. Sci., Polym. Phys. Ed.* **1985**, *23*, 275.
(41) Vrentas, J. S.; Duda, J. L.; Ling, H. C.; Hou, A. C. *J. Polym. Sci., Polym. Phys. Ed.* **1985**, *23*, 289.
(42) Yasunaga, H.; Ando, I. *Polymer Gels Networks* **1993**, *1*, 83.
(43) Martin, J. E. *Macromolecules* **1986**, *19*, 922.
(44) Bansil, R.; Pajevic, S.; Konak, C. *Macromolecules* **1990**, *23*, 3380.

MA9502314